

# DUAL-CANTILEVER AFM PROBE FOR COMBINING FAST AND COARSE IMAGING WITH HIGH-RESOLUTION IMAGING

M. Despont<sup>1)</sup>, H. Takahashi<sup>2)</sup>, S. Ichihara<sup>2)</sup>, Y. Shirakawabe<sup>2)</sup>, N. Shimizu<sup>2)</sup>, A. Inoue<sup>2)</sup>, W. Häberle<sup>1)</sup>, G.K. Binnig<sup>1)</sup>, and P. Vettiger<sup>1)</sup>

<sup>1)</sup> IBM Research, Zurich Research Laboratory, 8803 Rüschlikon, Switzerland

<sup>2)</sup> Seiko Instrument Incorporated, 563, Takatsuka Shinden, Matsudo-shi, Chiba 270-222, Japan

## ABSTRACT

This paper presents a new scanning probe concept based on an integrated dual-cantilever device, which has been designed to reduce the tip-wear problem. It consists of two cantilevers, one having a robust blunt tip, the other having a sharp tip. By means of integrated bimorph actuators, such a cantilever can be used to switch between coarse and fast imaging with the blunt tip, and high-resolution imaging with the sharp tip. Hence the delicate sharp tip is used only when high resolution is required, which greatly increases the probe's lifetime. A high-sensitivity, constricted piezoresistive strain sensor is used for high-resolution imaging. Imaging with the dual-cantilever probe has been demonstrated successfully.

## INTRODUCTION

Atomic force microscopy (AFM) [1] is the most widely used scanning probe technique for surface analysis and imaging in applications such as material research, biochemistry, quality control and metrology. Ultrahigh resolution, simplicity and ease of operation are the key features of the AFM. However, high resolution is strongly related to sharp tips with apex radii in the nanometer range. Depending on operating conditions and sample material, the sharpness of the tip can undergo considerable wear and, hence, greatly affect the tip's lifetime even for tips coated with a hard material such as diamond [2]. The tip-wear issue is even more serious with the newest AFM instruments, which feature very large and fast scanning capabilities. Instruments with scan ranges up to 800  $\mu\text{m}$  are already on the market [3]. The large scan range/low-resolution and small scan range/high-resolution options of such new instruments are very versatile operating conditions that allow one to zoom from the macro to the nanoscale. However tip wear is increased by the large and fast scanning modes, which negatively affects performance in the high-resolution mode. In an automated AFM metrology and inspection system, tip wear is also a serious issue in terms of measure reliability and because throughput is affected by frequent downtimes for probe exchange.

We present a new concept based on an integrated dual-cantilever/tip, which is specifically designed and fabricated to reduce tip wear significantly and hence increase the robustness of an AFM system [4]. The cantilever with the robust tip having a blunt apex is used for the large and fast scan mode; the second cantilever with a very sharp tip apex is used only when ultrahigh resolution in a small and slow scan mode is required. Integrated thermal bimorph actuation is used to switch between the two cantilevers/tips. The two modes of operation are illustrated in Fig. 1.  $z$ -actuation with bimorph effect has been demonstrated for an individual feedback actuator of an AFM cantilever with an actuation range of 500 nm [5]. The dual-cantilever concept also allows a faster and more robust probe approaching scheme. To avoid tip damage when the tip makes contact with the sample, a slow and careful approach is usually required. With the dual-cantilever probe, the approach is always made with the blunt tip, hence no special precautions are necessary.

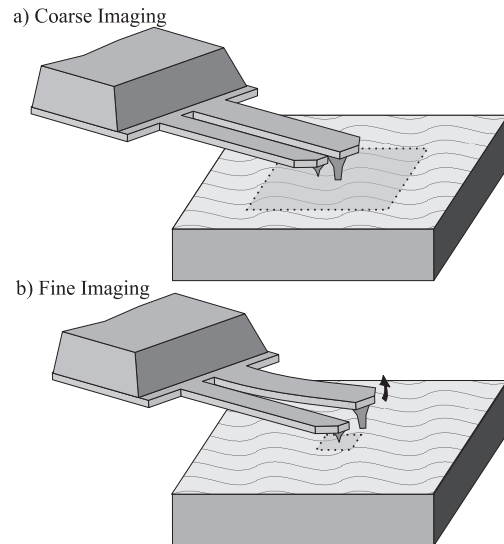


Figure 1: Concept of the dual cantilever. (a) Coarse, large and fast scan imaging is performed with the blunt tip (the sharp tip is not touching the sample). (b) After the blunt tip cantilever has been bent back with the integrated actuator, the sharp tip is brought into contact, and high-resolution imaging can be done on places of interest.

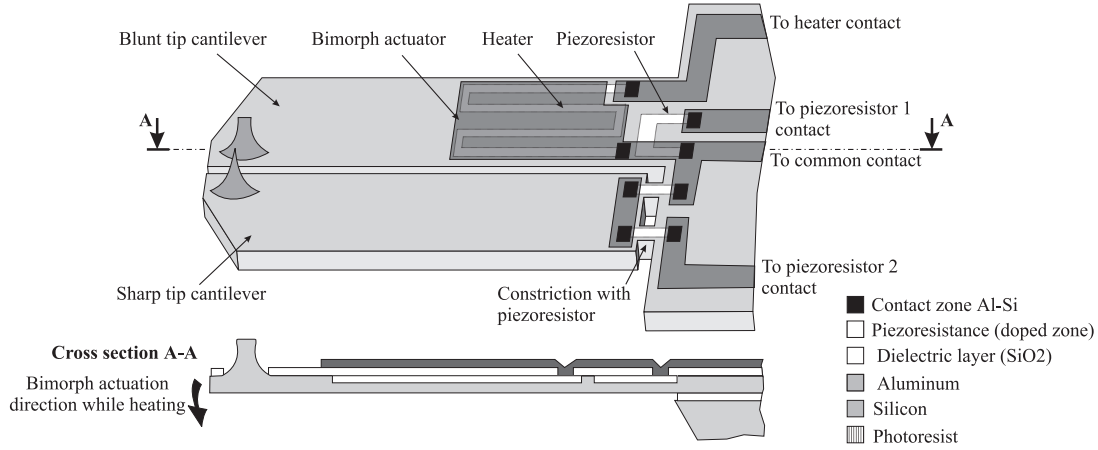


Figure 2: Schema and cross section of the dual-cantilever probe showing the various parts of the device.

### Design

Figure 2 shows a basic sketch of the dual-cantilever probe with a blunt tip and a sharp tip. Both have a piezoresistive deflection strain sensor. The sharp-tip cantilever has a laterally constricted piezoresistive sensor to increase sensitivity for high-resolution imaging. Constricted piezocantilevers have shown sensitivities as high as  $3 \times 10^{-5} \Delta R/R$  per nanometer for a stiff cantilever (30 - 40 N/m) used in dynamic AFM mode and  $6 \times 10^{-6}$  for a soft cantilever (3 - 5 N/m) used in contact mode [3,6]. The distance between the two tips is kept small to minimize the offset correction needed for the scanner while switching from one tip to the other. The tip heights are also different in order for the desired tip to make contact with the sample when no actuation is applied. The bimorph actuators are located on the blunt tip cantilever (the wider one) and the bimorph stack is performed by the silicon cantilever and a pad of another material deposited on top. Heating is provided by an integrated silicon-doped resistance underneath the pad. The  $z$ -actuation along the bimorph device can be calculated as follows (based on [7]):

$$\frac{d^2 z}{dx^2} = 6(a_{\text{Si}} - a_{\text{pad}}) \frac{t_{\text{pad}} + t_{\text{Si}}}{t_{\text{Si}}^2 k} (T - T_0),$$

$$k = 4 + 6 \frac{t_{\text{pad}}}{t_{\text{Si}}} + 4 \left( \frac{t_{\text{pad}}}{t_{\text{Si}}} \right)^2 + \frac{E_{\text{pad}}}{E_{\text{Si}}} \left( \frac{t_{\text{pad}}}{t_{\text{Si}}} \right)^3 + \frac{E_{\text{Si}}}{E_{\text{pad}}} \frac{t_{\text{Si}}}{t_{\text{pad}}}.$$

Where  $z$  is the vertical deflection at a position  $x$  along the bimorph pad.

The deflection at the end of the bimorph pad is

$$z_{\text{end\_pad}} = \frac{3L_{\text{pad}}^2}{t_{\text{Si}}^2 k} (a_{\text{Si}} - a_{\text{pad}}) (T - T_0) (t_{\text{pad}} + t_{\text{Si}}),$$

and the deflection angle at the same point is

$$\theta_{\text{end\_pad}} = \frac{6L_{\text{pad}}}{t_{\text{Si}}^2 k} (a_{\text{Si}} - a_{\text{pad}}) (T - T_0) (t_{\text{pad}} + t_{\text{Si}}).$$

Given a total deflection at the tip position of (assuming the deflection angle is small)

$$z_L = z_{\text{end\_pad}} + (L - L_{\text{pad}} - L_{\text{base}}) \theta_{\text{end\_pad}},$$

where  $z_L$  is the actuation range at the tip level,  $L_{\text{pad}}$  is the length of the bimorph pad,  $t_{\text{Si}}$  and  $t_{\text{pad}}$  are the thickness of the cantilever and the bimorph pad, respectively,  $\alpha_{\text{Si}}$  and  $\alpha_{\text{pad}}$  are the thermal expansion coefficients of silicon and the bimorph material pad,  $T_0$  and  $T$  the room and raised temperatures,  $L$  the length of the lever,  $L_{\text{base}}$  the distance between the cantilever base and the beginning of the bimorph pad, and, finally,  $E_{\text{Si}}$  and  $E_{\text{pad}}$  the Young's modulus of the silicon and the bimorph pad material, respectively.

Aluminum has been chosen as bimorph pad material mainly because of its compatibility with the chip fabrication. It also has a high thermal expansion coefficient mismatch with silicon ( $\alpha_{\text{Si}} = 2.5 \times 10^{-6}$  and  $\alpha_{\text{Al}} = 24 \times 10^{-6}$ ), which yields an efficient bimorph effect. On the other hand, its Young modulus is low and it has poor temperature stability (it oxidizes and reacts with silicon at low temperatures). For 350 °C, the actuation is 13  $\mu\text{m}$  ( $L_{\text{pad}} = 110 \mu\text{m}$ ,  $t_{\text{Si}} = 5 \mu\text{m}$ ,  $t_{\text{pad}} = 1 \mu\text{m}$ ,  $L = 300 \mu\text{m}$ ,  $L_{\text{base}} = 38 \mu\text{m}$ ,  $E_{\text{Si}} = 169 \text{ GPa}$ ,  $E_{\text{Al}} = 69 \text{ GPa}$ ), which is sufficient for our applications.

### Fabrication

Figure 3 shows the key process step at cross section A-A (see Fig. 2) for the dual-cantilever chip fabrication. Compared to a piezoresistive cantilever process, no additional process steps are necessary to fabricate the dual-cantilever probe. The initial substrate is a 4-inch silicon-on-insulator (SOI) wafer with a 10- $\mu\text{m}$ -thick,  $n$ -doped silicon membrane. The silicon tips are etched in the membrane with isotropic  $\text{SF}_6$ -based reactive ion etching (RIE) using a patterned thermal oxide layer as etching mask. Then the tips are sharpened by subsequent thermal oxidation. The blunt and the sharp tips are fabricated at the same time; a simple mask size difference is used to fabricate the two different kinds of tips as illustrated in Fig. 4, which also yielded a difference of tip heights. The next process step is to

define the cantilever geometry by  $\text{SF}_6/\text{O}_2$  RIE (Fig. 3a). The piezoresistor is fabricated by boron-ion implantation and subsequent thermal dopant activation. Then, a CVD silicon oxide is deposited (Fig. 3b). Contact zones are opened in the oxide layer with buffered fluoridric acid (BHF) followed by sputter deposition of a 1- $\mu\text{m}$ -thick aluminum layer. The bimorph pad and the wiring are patterned with a  $\text{H}_3\text{PO}_4/\text{CH}_3\text{COOH}/\text{HNO}_3/\text{H}_2\text{O}$ -based aluminum etch solution. Then a thermal treatment is performed to alloy the Si-Al contact (Fig. 3c). Afterwards, the backside oxide is opened with a BHF etch, whereas the front side is protected by a photoresist. The chip is released with a KOH etch using a chuck to protect the front side (Fig. 3d). The chips are kept attached to the wafer by this suspension's delineate in the silicon membrane, providing an easy way of releasing the chip from the wafer when fabrication has been completed. The last steps are to remove the buried oxide of the SOI wafer with BHF using the resist as front side protection and to strip the resist (Fig. 3e).

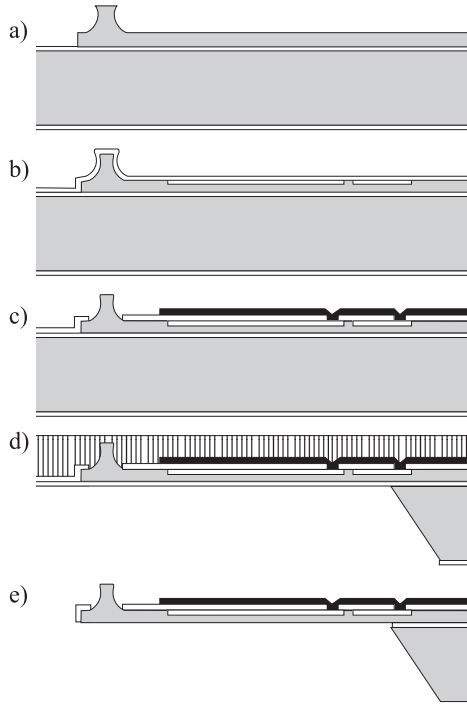


Figure 3: Process flow chart of key steps in the fabrication of the dual-cantilever chip. The cross section shown is the same as in Fig. 2 and uses the same pattern code for the various materials.

In the fabricated device, the bimorph stack consists of the silicon lever, a dielectric  $\text{SiO}_2$  layer, and the aluminum pad. Our calculations do not take the oxide layer into account. However, the  $\text{SiO}_2$  layer is relatively thin ( $\sim 400$  nm) and its thermal linear expansion

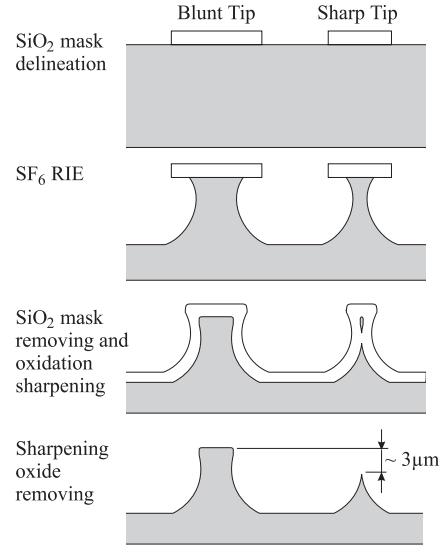


Figure 4: Process steps for the fabrication of the blunt and sharp tips.

coefficient is very close to that of silicon ( $\alpha_{\text{SiO}_2} = 0.5 \times 10^{-6}$ ,  $\alpha_{\text{Si}} = 2.5 \times 10^{-6}$ ), so this configuration has little influence on the bimorph effect (less than 10%). Moreover, the dielectric  $\text{SiO}_2$  layer covers the entire surface of both levers in order to achieve the same bending due to the stress of the Si- $\text{SiO}_2$  interface.

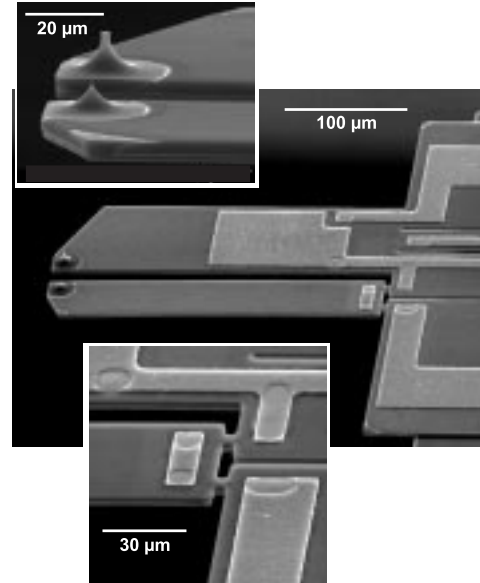
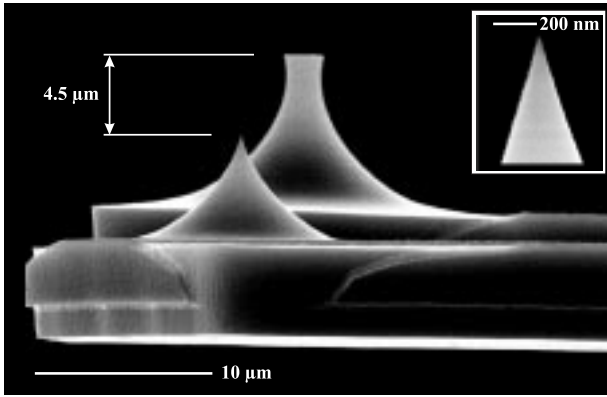


Figure 5: SEM image of a global view of the dual cantilevers. It can be compared directly with Fig. 2 for the different parts of the devices. Inset: detail of the dual tip and of the constricted piezoresistance.

Figure 5 shows a scanning electron micrograph of the fabricated dual-cantilever probe with a magnified view of the blunt and sharp tips and of the constricted piezoresistance. It can be compared directly with Figure 2 for the different parts of the device. The distance

between the two tips is 25  $\mu\text{m}$ . Figure 6 shows a side view of the two tips and a highly magnified view of the sharp tip apex. The difference of the tip-apex heights is approximately 4.5  $\mu\text{m}$ , which results from the tip height difference ( $\sim 3 \mu\text{m}$ ) and the cantilever bending difference ( $\sim 1.5 \mu\text{m}$ ). The sharp tip height and its apex radius were found to be homogeneous across the wafer. Within the 3-inch diameter of the wafer the tip height tolerance is better than 500 nm. The high aspect ratio of the last part of the tip and its small apex radius ( $< 20 \text{ nm}$ ) are suitable for high-resolution imaging application. The blunt tip has a radius of  $\sim 900 \text{ nm}$ .



Figures 6: SEM image of the two-tip area showing the different tip shapes, tip heights and the bending difference between the two cantilevers. The total tip apex height difference is  $\sim 4.5 \mu\text{m}$ . Inset: detail of the sharp tip apex, showing the high aspect ratio of the tip and its small radius ( $< 20 \text{ nm}$ ).

## Experiments

Experiments were performed with a SPI3800N Seiko Instrument Inc. AFM system. Figure 7 shows the measured tip deflection versus the electrical power used for the bimorph actuation. The dimensions of the cantilever are the same as those given in the design section. The measured heater resistance at low power is 4.9 k $\Omega$ . The labels  $z_b$  and  $z_s$  denote the deflection of the blunt and sharp tips respectively. An estimation of the temperature scale is also given, using as reference the power needed to start melting the aluminum of the bimorph pad ( $\sim 660^\circ\text{C}$ ), which has been observed at 110 mW. The theoretical  $z_b$  value given by the equations above was also plotted using the estimated temperature to calculate the corresponding actuation. Some thermal crosstalk between the two cantilevers produce a small actuation of the sharp tip cantilever ( $z_s$ ). It is probably also due to a bimorph effect, but it is 20 times smaller than the actuation of the blunt tip. When the bimorph is heated, an additional remnant stress is observed in the bimorph. This is illustrated by the curve  $\Delta_0$ , which is the zero power blunt tip height generated by the remnant

stress after first actuation with the given power. Additional stress is built up in the bimorph stack, most

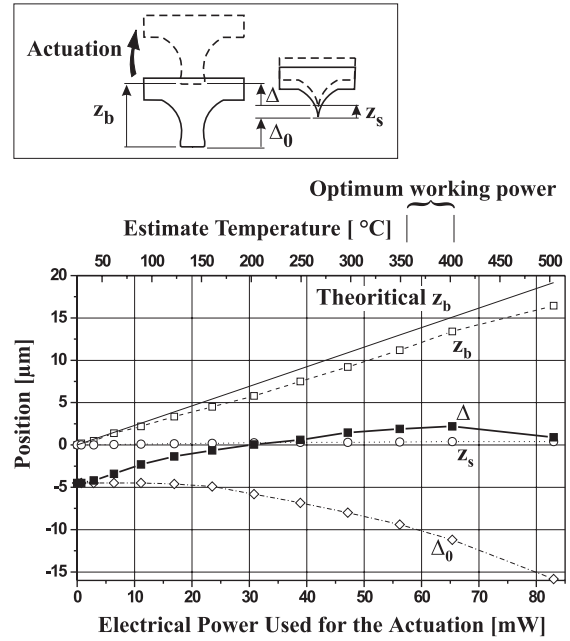


Figure 7: Characteristic of the bimorph actuator of the dual-cantilever probe of Fig. 5. The  $z$ -position is plotted versus the bimorph actuation heating power as shown in the sketch.  $z_b$  is the blunt tip actuation,  $z_s$  is the actuation of the sharp tip by thermal crosstalk,  $\Delta_0$  is the zero power position of the blunt tip after first time operation, and  $\Delta$  is the final tip height difference ( $\Delta = z_b - z_s - \Delta_0$ ). Estimated bimorph actuator temperature and, theoretical blunt tip actuation is also shown.

probably due to aluminum oxidation while heating. Finally,  $\Delta$  is the real measured tip height difference ( $\Delta = z_b - z_s - \Delta_0$ ) versus the bimorph operating power. It has a maximum at  $\sim 65 \text{ mW}$ , which yielded the optimum operating point switching from  $-11.2 \mu\text{m}$  at 0 mW to  $+2.2 \mu\text{m}$  at 65 mW. The values measured here are for this specific design, however  $\Delta$  can be changed to any operating requirement by changing the bimorph design.

The frequency response and sensitivity of both cantilevers have been measured with optical and piezoresistive detection methods. Typical measured resonant frequencies are 49.58 kHz for the sharp tip and 67.31 kHz for the blunt tip cantilever. A mechanical coupling between the two cantilever has been observed. This occurs through the silicon membrane at the base of the cantilevers because the edge of the chip body is slightly recessed ( $\sim 20 \mu\text{m}$ , see Fig. 3d). Another observation made in this experiment is that the bimorph heater can perfectly play the role of piezoresistance sensor during operation with the blunt tip. Hence the number of electrical connections can be minimized.

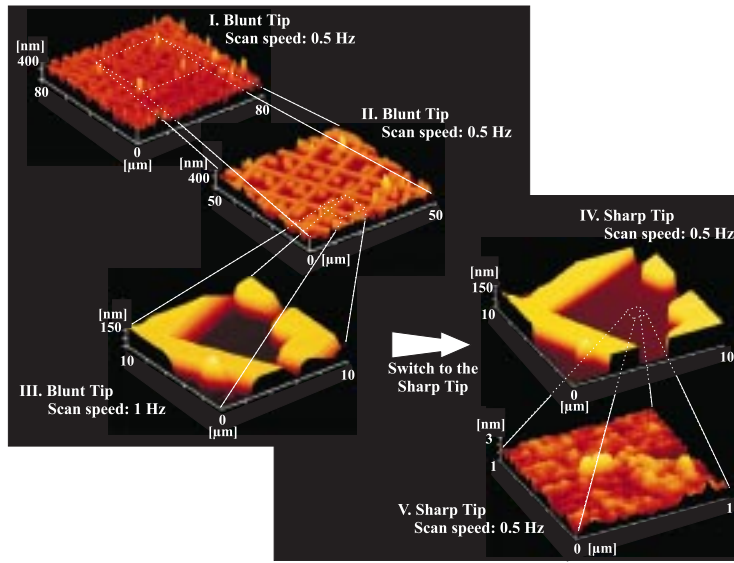


Figure 8: Typical AFM imaging sequence with the dual-cantilever chip. (I), (II), (III) show fast scan rate images taken with the blunt tip at progressively greater magnifications to locate places of interest. After switching to the sharp tip, we obtain the high-resolution images shown in (IV) and (V). (III) and (IV) are images of the same sample zone but taken with two different tips. The sample is a 100-nm-thick SiO<sub>2</sub> structure on a silicon substrate.

Deflection sensitivities of  $6.80 \times 10^{-6}$ ,  $2.06 \times 10^{-6}$ , and  $1.62 \times 10^{-6}$   $\Delta R/R$  per nanometer for the sharp tip cantilever with constricted piezoresistor, the blunt tip cantilever piezoresistor, and the bimorph resistance, respectively, have been measured. A constricted piezoresistor has a sensitivity 3 times higher than a nonconstricted piezoresistor.

Figure 8 summarizes a typical measurement sequence performed with the dual-cantilever probe. The sample used is a 100-nm-thick silicon oxide pattern on a silicon substrate, with the large square pattern being  $10 \times 10 \mu\text{m}^2$ . The experiment was done in contact mode using the piezoresistive sensing of the cantilever in operation. After the approach process of the blunt tip cantilever, image I was taken. It is a fast and large scan (scanning speed: 0.5 Hz, scan length:  $80 \mu\text{m}$ ). A second and third imaging step (images II and III) were performed at the same scan speed and still with the blunt tip to the precise zone of interest. The low lateral resolution of image III is determined by the blunt tip. Switching to the sharp cantilever is done by the following operating sequence: (a) slightly retracting the chip from the sample by means of the piezoscanner, (b) the blunt tip is switched back with the bimorph actuator, (c) the offset corresponding to the tip distance is corrected with the piezoscanner to get the sharp tip at the same sample position as the blunt tip, and (d) a low-speed reapproach is performed with the sharp tip. Then image IV was taken, which shows the same area as displayed in image III, but imaged with the sharp tip. A much higher lateral resolution can be observed. Finally a high-resolution image (image V) shows the very high lateral and vertical resolution of the sharp tip cantilever. Such a resolution would probably not have been possible if all the images taken during this experiment had been made by the sharp tip only, because it would most likely have been damaged before image V was taken.

Many similar experiments have been performed without damage or wear to the sharp tip using optical or piezoresistive detection. Very fast and careless approaches have also been performed, and the sharp tip suffered no damages either.

Another important point is the temperature of the tip apex when the bimorph stack is heated. For certain applications a hot tip is undesirable, especially for temperature-sensitive samples such as biological material. For that purpose sharp tip bending due to thermal crosstalk between the two cantilevers has been measured on probes where the sharp tip cantilever is also coated with aluminum. An average temperature of the sharp tip cantilever below  $40^\circ\text{C}$  when the heater is at  $400^\circ\text{C}$  (65 mW) has been estimated from its bending, with the sharp tip apex temperature being even lower. This result suggests that for most applications the temperature of the sharp tip should not be a problem, but further investigations are necessary to confirm this finding.

## Discussion

The main problem that occurred during imaging with the dual-cantilever chip using the sharp tip is that the blunt tip can sometimes suddenly make contact with the sample surface. The tip height difference in this condition is only  $2.2 \mu\text{m}$  for a tip distance of  $25 \mu\text{m}$ . If the sample is tilted relative to the probe or the sample has tall structures,  $2.2 \mu\text{m}$  is not enough to prevent the blunt tip from touching the surface. This situation is mainly due to the remnant stress in the bimorph stack after heating, which decreases the tip height difference drastically when the sharp tip is activated. This can be improved by various means. Reducing the tip distance will avoid the sample-probe tilt problem. A tip distance in the  $15 \mu\text{m}$  range is feasible. The bimorph actuation can also be increased. One possibility is to modify the



actuator-cantilever geometrically, e.g. to use a thicker and/or longer aluminum pad, and a thinner and/or longer cantilever. Dual-cantilever probes with a longer lever and longer bimorph pad have been fabricated in the same batch.

Figure 9 shows the actuation efficiency of a 400- $\mu\text{m}$ -long cantilever with a 235- $\mu\text{m}$ -long aluminum pad. The tip height difference is  $-8.4\text{ }\mu\text{m}$  at 0 mW and  $8.9\text{ }\mu\text{m}$  at 57 mW, which in both cases is a sufficient difference for operating the probe. Another possibility is to use a more suitable material than aluminum having a better optimum between its Young modulus, its linear thermal expansion coefficient, its deposition stress, and its thermal stability (allowing a higher operating temperature without building permanent stress in the bimorph stack). However, of the commonly used materials, aluminum has a strong bimorph effect when used with silicon. Only copper, nickel, and cobalt have similar efficiency, and that of zinc is considerably better ( $\sim 1.5\times$ ), but their thermal stability at operating temperature and deposition stress have yet to be investigated. Some of their alloys or oxides may also be interesting material.

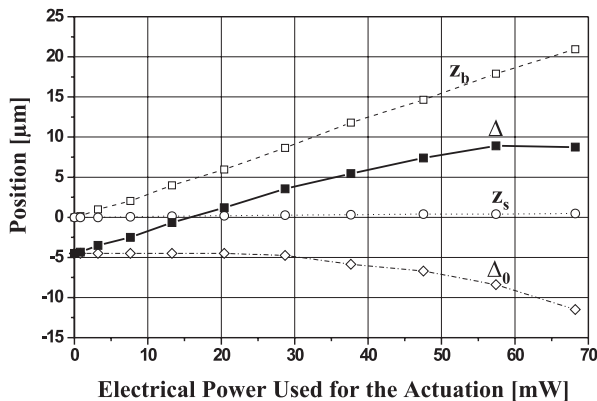


Figure 9: Characteristic of the bimorph actuator of a dual-cantilever, which is 400- $\mu\text{m}$ -long and has a 235- $\mu\text{m}$ -long bimorph pad. Actuation efficiency is drastically improved.

The piezoresistive-based dual-cantilever concept has also been demonstrated for optical detection, however, it was inconvenient to manually switch the laser-beam between the two levers. This procedure is difficult to automate. A possibility would be to keep the laser focus on only one lever (the sharp tip cantilever) and to use the mechanical coupling observed between the levers to be able to read out the deflection of the second lever (blunt tip). Such coupling can be optimized for an optical dual-cantilever probe.

## CONCLUSION

We successfully demonstrated our dual-cantilever AFM probe concept for combining fast and coarse imaging with high-resolution imaging. It has been designed to reduce tip wear. Our experiments have confirmed the robustness of the dual cantilever concept, no tip damage was observed, even with careless operation. It is a very attractive concept for AFM imaging systems because it features robustness even with high speed operation and a large scan range, which is critical for tip wear. It also allows reproducible measurements over a long time range and reduces the system downtime for automated AFM-based metrology system. Both optical and piezoresistive self-sensitive detection have been used and demonstrated.

## ACKNOWLEDGMENTS

We are pleased to acknowledge the contributions of the MJ group and the clean room team of the Seiko Instrument Inc. Takatsuka Unit, as well as the Nano and Micromechanics group of the IBM Zurich Research Laboratory. Special thanks for the support of H. Rohrer, K. Kümmerle, and C. Takahata.

## REFERENCES

- [1] G. Binnig, Ch. Gerber, and C.F. Quate, J. Appl. Phys. Lett. **53**, 1044 (1988).
- [2] A.G. Khurshudov, K. Kato, and H. Koide, "Wear of AFM Diamond Tip Sliding Against Silicon", Wear 203-204, (1997), 22-27.
- [3] Seiko Instruments Inc., "Nanoptics Specification Brochure", 1998.
- [4] G.K. Binnig, J. Brugger, W. Haeberle, H. Rohrer, and P. Vettiger, "Novel Cantilever Structures", PCT Publication No. WO97/34122, published 18 September 1997.
- [5] D. Lange, T. Akiyama, C. Hagleitner, A. Tonin, H.R. Hidber, P. Niedermann, U. Staufer, N.F. de Rooij, O. Brand, and H. Baltes, "Parallel Scanning AFM with On-Chip Circuitry in CMOS Technology", Technical Digest 12th IEEE Int'l Micro Electro Mechanical Systems Conf. "MEMS'99", Orlando, FL, January 1999, IEEE, Piscataway, 1999, pp. 447-452.
- [6] M.I. Lutwyche, C. Andreoli, G. Binnig, J. Brugger, U. Drechsler, W. Haeberle, H. Rohrer, H. Rothuizen, P. Vettiger, G. Yaraliglu, and C. Quate "5x5 2D AFM Cantilever Arrays: A First Step Towards a Terabit Storage Device", Sensors & Actuators A, 73 (1999), 89-94.
- [7] W.C. Young, "Roak's Formulas for Stress & Strain", 6th ed., McGraw-Hill, 1989.